

## Tetraviologen calix[4]resorcine as a mediator of the electrochemical reduction of $[\text{PdCl}_4]^{2-}$ for the production of $\text{Pd}^0$ nanoparticles

Vitaly V. Yanilkin,\* Gulnaz R. Nasybullina, Albina Yu. Ziganshina, Irek R. Nizamiev, Marsil K. Kadirov, Dmitry E. Korshin and Alexander I. Kononov

A. E. Arбузов Institute of Organic and Physical Chemistry, Kazan Scientific Centre of the Russian Academy of Sciences, 420088 Kazan, Russian Federation. Fax: +7 843 275 2253; e-mail: yanilkin@iopc.ru

DOI: 10.1016/j.mencom.2014.03.015

Tetraviologen calix[4]resorcine was used as a mediator for the electrochemical reduction of  $[\text{PdCl}_4]^{2-}$ . The mediator facilitates the complex reduction to 0.6 V on a glassy carbon electrode, which results in the formation of palladium metal nanoparticles with average diameters of 160 to 850 nm.

Octacationic tetraviologen calix[4]resorcine ( $\text{MVCA}^{8+}$ ) effectively binds multicharged anions through the electrostatic or donor–acceptor interaction of viologen units with anions or donor centers.<sup>1–7</sup> These intermolecular interactions weaken after the reduction of the viologen units to a radical cation or neutral state. However, new non-covalent intermolecular interactions of MVCA appear after the reduction: (i)  $\pi$ -dimerization of the radical cations of the viologen units and (ii) hydrophobic binding of guests by the calixresorcine platform. The reverse oxidation of the viologen units to the original dication state leads the system to return to its original state. The management of these intermolecular interactions through the electrochemical reactions of viologens, the length of the hydrophobic tails of the resorcinarene platform, the media and nature of the substrate allowed us to create different electrochemically controlled systems in which the reversible molecular switching of a molecular system to a supramolecular system,<sup>2</sup> a monomer to a polymer,<sup>3</sup> and one supramolecular system to another<sup>4–8</sup> occur.  $[\text{PdCl}_4]^{2-}$  was used in the study of  $\text{MVCA-C}_5^{8+}$  to create new electrochemically controlled systems.  $[\text{PdCl}_4]^{2-}$  is easily formed from  $\text{PdCl}_2$  in the presence of chloride ions.<sup>9</sup> It undergoes two-electron reduction to produce solid or dispersed palladium metal.<sup>9</sup> The reduction of  $\text{PdCl}_2$  is more difficult than the reduction of  $\text{MVCA-C}_5^{8+}$  on a glassy carbon (GC) electrode in DMF solution.<sup>9</sup> Accordingly, it is possible to reduce the viologen units of  $\text{MVCA}^{8+}$  without affecting  $[\text{PdCl}_4]^{2-}$  and to create electroswitchable systems similar to the previous systems. We studied the  $\text{MVCA-C}_5^{8+} + [\text{PdCl}_4]^{2-}$  system in 60% aqueous DMF and obtained unexpected results.

The cyclic voltammograms (CVs) of  $\text{MVCA-C}_5^{8+}$  recorded on the GC electrode in 60% aqueous DMFA/0.1 M NaCl media exhibit two typical<sup>1–7,11,12</sup> reduction peaks  $C_1$  and  $C_2$  ( $E_{\text{p,red}}^1 = -0.45$  V,  $E_{\text{p,red}}^2 = -0.93$  V) and two re-oxidation peaks  $A_1$  and  $A_2$  ( $E_{\text{p,redox}}^1 = -0.37$  V,  $E_{\text{p,redox}}^2 = -0.76$  V) (see Figure S1, Online Supplementary Materials). The reduction of the viologen units of  $\text{MVCA-C}_5^{8+}$  to a radical cation state occurs at the first step with the formation of a tetra(radical cation)  $\text{MVCA-C}_5^{4+}$  (Scheme S1). The fully reduced neutral  $\text{MVCA-C}_5^0$  is produced at the second step. The first reduction peak is diffusion controlled, and all of the other peaks have an adsorption nature; that is, octacationic  $\text{MVCA}^{8+}$  does not cover the electrode surface, while  $\text{MVCA-C}_5^{4+}$  and  $\text{MVCA-C}_5^0$  adsorb the electrode largely.

The CV of  $\text{PdCl}_2$  (1.5 mM) in 0.1 M  $\text{NaClO}_4$  solution shows a broad irreversible reduction peak  $C_3$  at the first reduction peak potentials of  $\text{MVCA}^{8+}$  ( $E_{\text{p,red}}^3 = -0.59$  V) (Figure S2). The re-oxidation peak  $A_3$  of palladium metal ( $\text{Pd}^0$ )<sub>n</sub> is highly extended

and observed as a gradual increase in the Faraday current in the anodic potential region ( $E_{\text{p,redox}}^3 \approx +0.80$  V). In the region of more cathode potentials, the rise of the reduction current of the background solution is observed, which begins at a potential of  $-1.3$  V in the absence of  $\text{PdCl}_2$ . Hydrogen overvoltage at palladium<sup>13</sup> is lower than that at GC<sup>14</sup> by 0.42 V. Apparently, the easier background reduction in the presence of  $\text{PdCl}_2$  is due to the easier reduction of water on palladium with the formation of hydrogen (molecular or atomic) adsorbed on ( $\text{Pd}^0$ )<sub>n</sub> and oxidized at the peak  $A_4$  ( $E_{\text{p,redox}}^4 \approx -0.45$  V).

The addition of sodium chloride to a solution of  $\text{PdCl}_2$  does not affect the morphology of CV, the shift of the reduction peak is only observed, as described elsewhere<sup>9</sup> (Figure S2). Replacement of the supporting electrolyte by 0.1 M NaCl causes the largest shift of the irreversible reduction peak  $[\text{PdCl}_4]^{2-}$  ( $E_{\text{p,red}} = -0.91$  V). This peak is located between two reduction peaks of  $\text{MVCA}^{8+}$ . Metal particles ( $\text{Pd}^0$ )<sub>n</sub> formed by the reduction of  $[\text{PdCl}_4]^{2-}$  are oxidized in the form of a clear peak at  $E_{\text{p,redox}}^3 = +0.66$  V.

The mixing of  $\text{MVCA-C}_5^{8+}$  (0.5 mM) and  $[\text{PdCl}_4]^{2-}$  results in a decrease in the reduction peak  $C_3$  of  $[\text{PdCl}_4]^{2-}$ , the disappearance of the re-oxidation peak  $A_4$  and the appearance of a new reduction peak  $C_1'$  with the less cathodic potential  $E_{\text{p,red}}^{1'} = -0.33$  V (Figure 1). The height of this peak increases with the concentration of  $\text{PdCl}_2$ . The re-oxidation peak of ( $\text{Pd}^0$ )<sub>n</sub> is recorded at a significantly lower anode potential if the reverse scan starts from the potential  $C_1'$  (Figure S3). Consequently,  $[\text{PdCl}_4]^{2-}$  is reduced easier to 0.6 V at the potential of the new peak  $C_1'$  in the presence

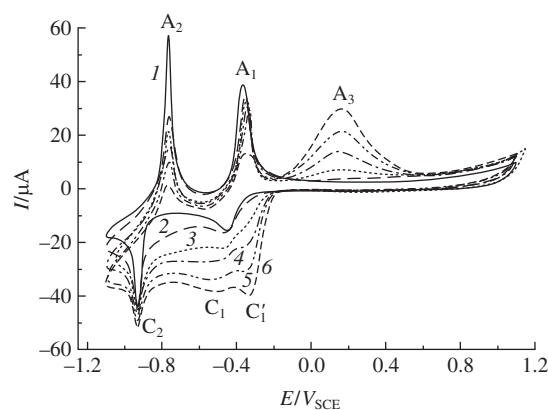
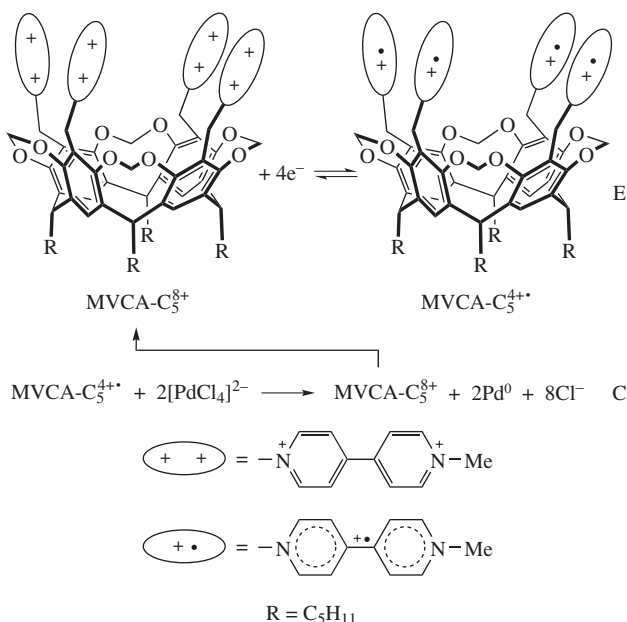


**Figure 1** CV of the  $\text{MVCA-C}_5^{8+} + \text{PdCl}_2$  system in 60% DMF/0.1 M NaCl media using a GC electrode at a scanning rate of  $100 \text{ mV s}^{-1}$ ;  $C(\text{MVCA-C}_5^{8+}) = 0.5 \text{ mM}$ ,  $C(\text{PdCl}_2) = (1) 0$ , (2) 0.5, (3) 1.0, (4) 1.5, (5) 2.0 and (6) 2.5 mM.



**Scheme 1** Mediator electrochemical reduction of  $[\text{PdCl}_4]^{2-}$ .

of  $\text{MVCA-C}_5^{8+}$ . The re-oxidation peak of  $(\text{Pd}^0)_m$  becomes slightly negative ( $E_{\text{p, reox}}^3 = 0.18\text{--}0.20$  V) if the reverse scan begins at the potential of the first reduction peak of  $\text{MVCA-C}_5^{8+}$  (Figure S4). These facts can be interpreted as  $[\text{PdCl}_4]^{2-}$  is reduced by the tetra-(radical cation)  $\text{MVCA-C}_5^{4+}$  in the solution layer at the electrode with the formation of  $(\text{Pd}^0)_m$  in the bulk solution (Scheme 1). These particles have a smaller size ( $m < n$ ), and therefore easier oxidize.

There is a definite relationship between the oxidation potential and the size of metal nanoparticles:<sup>15</sup>

$$E_{\text{np}}^{0'} = E^{0'} - a/r_{\text{np}},$$

where  $E_{\text{np}}^{0'}$  is the formal oxidation potential of nanoparticles;  $E^{0'}$  is the formal oxidation potential of the bulk metal;  $a$  is a coefficient including a function of the surface energy, atomic weight, the metal density and Faraday constant;  $r_{\text{np}}$  is the radius of the nanoparticle. Palladium particles formed during the mediatory reduction are oxidized as a single peak at lower anode potentials. Hence, these particles have a similar size, which is smaller than that for particles produced by the direct reduction of  $[\text{PdCl}_4]^{2-}$  on the GC electrode ( $m < n$ ).

Evidence for the mediatory reduction of  $[\text{PdCl}_4]^{2-}$  is the result of an enlarged electrolysis at GC cloth at the potential of the first reduction of  $\text{MVCA-C}_5^{8+}$  ( $E = -0.60$  V). The solution properties were monitored by CV on the indicator GC electrode, which was used before for the recording of all previous CV curves. Note that, in this case, for unknown reasons, the peak  $C_1'$  is bifurcated on the CV of the mixture  $[\text{PdCl}_4]^{2-}$  (1.5 mM) +  $\text{MVCA-C}_5^{8+}$  (0.5 mM) before electrolysis, while the oxidation peak of  $(\text{Pd}^0)_m$  is shifted to more anodic area ( $E_{\text{p, reox}}^3 = +0.41$  V) (Figure S5). During the electrolysis, the solution remains homogeneous and becomes dark brown. The violet color of the intermolecular  $\pi$ -dimerized viologen radical cations occurs only after passing 2 F per mole of  $[\text{PdCl}_4]^{2-}$ . From this it follows that  $\text{MVCA-C}_5^{4+}$  reduces  $[\text{PdCl}_4]^{2-}$  to  $\text{Pd}^0$  with  $\sim 100\%$  current efficiency in the bulk solution yield. On the CV curves, there are no the reduction peaks of  $[\text{PdCl}_4]^{2-}$  ( $C_1'$  or  $C_3$ ), while the reduction and re-oxidation peaks of  $\text{MVCA-C}_5$  are recorded (Figure S6). In the anode region, two peaks of the oxidation of  $(\text{Pd}^0)_m$  are observed: a poorly defined peak at  $E_{\text{p, reox}} = +0.21$  V and an intense peak at almost the same potential as in the CV before electrolysis ( $E_{\text{p, reox}}^3 = +0.46$  V). Their intensities and potentials are almost the same as that for the individual

$\text{MVCA-C}_5$ . In the anodic area, the oxidation peak of  $(\text{Pd}^0)_m$  is observed at almost the same potential as that on the CV before the electrolysis ( $E_{\text{p, reox}}^3 = +0.46$  V). The intensity of this peak increases until a certain limit with increasing the residence time of the electrode in the solution without applying potential before the recording of CV (Figure S7). The peak potential does not change. Obviously, the solution after electrolysis contains  $(\text{Pd}^0)_m$  with the same size as the palladium particles adsorbed on the surface of the generating electrode. They are slowly adsorbed on the indicator GC electrode without changing the size; that is, they are stabilized and do not stick together within minutes. These particles are resistant to oxygen. The CV curves remained unchanged after bubbling air for 10 min through the solution and then an inert gas to remove oxygen (Figure S8). According to dynamic light scattering, the average sizes of the  $(\text{Pd}^0)_m$  nanoparticles are 160 and 850 nm (Figure S9). The latter type of particles is predominant; the proportion is 96%, while the smaller particles are present in minor amounts in solution (4%). Apparently, the peak  $E_{\text{p, reox}}^3 = +0.46$  V corresponds to the oxidation of the particle with a size of 850 nm, and the peak  $E_{\text{p, reox}} = +0.21$  V is associated with the oxidation of 160 nm particles. The reverse oxidation at  $E = +0.6$  V by passing the same amount of electricity leads to the initial solution according to CV (Figure S10); that is, the electrogenerated  $\text{Pd}^0$  exists in the solution and the GC cloth in the form of nanoparticles, which are quantitatively oxidized to the original  $[\text{PdCl}_4]^{2-}$  at +0.6 V.

A similar cycle of the reduction ( $-1.0$  V) and oxidation ( $+0.6$  V) of  $[\text{PdCl}_4]^{2-}$  in the absence of the calixresorcine also leads to the initial solution. However, in this case, the palladium particles obtained are larger.  $\text{Pd}^0$  is deposited on the generating electrode; therefore, the CV does not detect any palladium particles in the solution (Figures S11–S13).

Note that the metal nanoparticles produced by the mediatory reduction stick together during prolonged standing in the solution (24 h or more) and settle to the bottom while the solution becomes decolorized. The precipitate was separated from the solution by centrifugation, washed with water and dispersed into water by sonication. The resulted solution was transferred onto a substrate (mica); then, the water was evaporated and the metal particles were studied using an atomic force microscope (AFM). The AFM image shown in Figure 2 demonstrates that the metal particles of size from 45 to 220 nm are arranged on the surface. Moreover, larger particles are formed by the agglomeration of smaller particles.

We showed the homogenous mediator electrochemical reduction of  $[\text{PdCl}_4]^{2-}$  to form stable  $(\text{Pd}^0)_m$  nanoparticles dissolved in 60% DMF and adsorbed on the GC electrode. Usually, metal complexes are used to catalyze the oxidation or reduction of organic compounds. The singularity of this system is that the organic compound catalyzes the reduction of the metal complex. In the test system, the mediator is  $\text{MVCA-C}_5^{8+}$ , and the active form

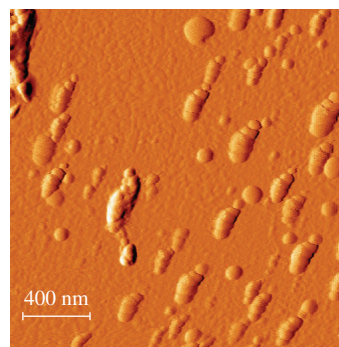


**Figure 2** AFM image of the  $\text{Pd}^0$  nanoparticles deposited onto a mica surface by the solvent evaporation method.

is MVCA-C<sub>5</sub><sup>4+</sup>. Apparently, the reduction mediator rate is quite high, so the reduction peak of MVCA-C<sub>5</sub><sup>8+</sup> is shifted toward the less cathodic potentials (C<sub>1</sub>' peak). Tetra(radical cation) MVCA-C<sub>5</sub><sup>4+</sup> could potentially be a donor of four electrons. Its donor properties retain during the donation of electrons; that is, MVCA-C<sub>5</sub><sup>4+</sup>, MVCA-C<sub>5</sub><sup>5+3+</sup>, MVCA-C<sub>5</sub><sup>6+2+</sup> and MVCA-C<sub>5</sub><sup>7+1+</sup> have the same ability to give electrons. It is unique for organic compounds because the donor ability usually decreases with the donating of electrons. The changes in the <sup>1</sup>H NMR spectrum of MVCA-C<sub>5</sub><sup>8+</sup> in the presence of [PdCl<sub>4</sub>]<sup>2-</sup> indicate the binding of the dianion with the macrocycle. A downfield shift of the H<sup>9</sup> proton and an upfield shift of the axial proton H<sup>8a</sup> are observed (Figure S14). When the two [PdCl<sub>4</sub>]<sup>2-</sup> bounded by the resorcinarene cavity, tetra(radical cation) MVCA-C<sub>5</sub><sup>4+</sup> have the resources to the full reduction of [PdCl<sub>4</sub>]<sup>2-</sup> with the formation of Pd<sup>0</sup>-Pd<sup>0</sup> and stabilization of these donor particles by the donor-acceptor interaction with four viologen acceptor units.

The electrochemical reduction of [PdCl<sub>4</sub>]<sup>2-</sup> directly on the electrode surface to form palladium metal is well known. Electrochemical processes for the preparation of all-metal palladium,<sup>9</sup> palladium on carbon,<sup>9</sup> and palladium nanoparticles at short electrolysis<sup>16–19</sup> were described. However, all these particles are deposited on the electrode surface. Problems arise in obtaining electrochemical palladium nanoparticles in solution. It is necessary to avoid the precipitation of palladium on the electrode. The use of traditional approaches is difficult or almost impossible because the reduction of [PdCl<sub>4</sub>]<sup>2-</sup> to Pd<sup>0</sup> on the deposited palladium occurs more easily than on a pure carbon electrode. For this reason, little attention is paid to the electrochemical production of fine (nanosized) palladium in solution. However, the colloidal solutions of palladium nanoparticles (particle size of 1–1000 nm) are well known.<sup>9</sup> Palladium nanoparticles are of great interest due to their high selective catalytic properties in many processes of the reduction, oxidation and coupling of organic compounds. These particles are mainly obtained by the chemical reduction of Pd<sup>II</sup> compounds. Monodisperse palladium nanoparticles (1–10 nm) were chemically prepared using different types of matrices, including polymers.<sup>20–23</sup> We did not use such methods in this work. Therefore, the particles obtained have sufficiently large size; after the removal of resorcinarene and solvent from the media, the polydisperse particles were isolated. However, the mediatory electrochemical reduction of [PdCl<sub>4</sub>]<sup>2-</sup> transfers the reduction process from the electrode surface into the bulk solution and minimizes the deposition of metal on the electrode, which makes the electrochemical process similar to a chemical one. Accordingly, it opens the possibility of the electrochemical production of the monodisperse nanoparticles of palladium with a specific size in solution using a stabilizing matrix.

This work was supported by the Russian Foundation for Basic Research (grant nos. 12-03-00379 and 14-03-00405).

#### Online Supplementary Materials

Supplementary data associated with this article can be found in the online version at doi:10.1016/j.mencom.2014.02.015.

#### References

- 1 A. Yu. Ziganshina, S. V. Kharlamov, E. Kh. Kazakova, Sh. K. Latypov and A. I. Konovalov, *Mendeleev Commun.*, 2007, 145.
- 2 A. Yu. Ziganshina, S. V. Kharlamov, D. E. Korshin, R. K. Mukhitova, E. Kh. Kazakova, Sh. K. Latypov, V. V. Yanilkin and A. I. Konovalov, *Tetrahedron Lett.*, 2008, **49**, 5312.
- 3 G. R. Nasybullina, V. V. Yanilkin, A. Y. Ziganshina, V. I. Morozov, E. D. Sultanova, D. E. Korshin, V. A. Milyukov, R. P. Shekurov and A. I. Konovalov, *Elektrokhimiya*, in press.
- 4 A. Yu. Ziganshina, G. R. Nasybullina, V. V. Yanilkin, N. V. Nastapova, D. E. Korshin, Yu. S. Spiridonova, R. R. Kashapov, M. Gruner, W. D. Habicher, A. A. Karasik and A. I. Konovalov, *Russ. J. Electrochem.*, 2014, **50**, 142 (*Elektrokhimiya*, 2014, **50**, 158).
- 5 G. R. Nasybullina, V. V. Yanilkin, N. V. Nastapova, A. Yu. Ziganshina, D. E. Korshin, Yu. S. Spiridonova, A. A. Karasik and A. I. Konovalov, *Russ. Chem. Bull., Int. Ed.*, 2012, **61**, 2295 (*Izv. Akad. Nauk, Ser. Khim.*, 2012, **61**, 2274).
- 6 G. R. Nasybullina, V. V. Yanilkin, N. V. Nastapova, D. E. Korshin, A. Yu. Ziganshina and A. I. Konovalov, *J. Inclusion Phenom. Macrocycl. Chem.*, 2012, **72**, 299.
- 7 V. V. Yanilkin, A. R. Mustafina, A. S. Stepanov, N. V. Nastapova, G. R. Nasybullina, A. Yu. Ziganshina, S. E. Solovieva and A. I. Konovalov, *Russ. J. Electrochem.*, 2011, **47**, 1082 (*Elektrokhimiya*, 2011, **47**, 1160).
- 8 D. E. Korshin, N. V. Nastapova, S. V. Kharlamov, G. R. Nasybullina, T. Yu. Sergeeva, E. G. Krasnova, E. D. Sultanova, R. K. Mukhitova, Sh. K. Latypov, V. V. Yanilkin, A. Yu. Ziganshina and A. I. Konovalov, *Mendeleev Commun.*, 2013, **23**, 71.
- 9 N. V. Korovin, *Korroziionnye i elektrokhimicheskie svoistva palladiya (Corrosion and Electrochemical Properties of Palladium)*, Metallurgiya, Moscow, 1976 (in Russian).
- 10 D. G. Yakhvarov, R. M. Kagirov, I. Kh. Rizvanov, V. I. Morozov and O. G. Sinyashin, *Mendeleev Commun.*, 2009, 190.
- 11 C. Peinador, E. Roman, K. Abboud and A. E. Kaifer, *Chem. Commun.*, 1999, 1887.
- 12 E. Roman, M. Chas, J. M. Quintela, C. Peinador and A. E. Kaifer, *Tetrahedron*, 2002, **58**, 699.
- 13 L. I. Antropov, *Teoreticheskaya elektrokhimiya (Theoretical Electrochemistry)*, Vysshaya Shkola, Moscow, 1965 (in Russian).
- 14 T. Erdey-Grüz and H. Wick, *Z. Phys. Chem.*, 1932, **162A**, 53.
- 15 W. J. Plieth, *J. Phys. Chem.*, 1982, **86**, 3166.
- 16 M. S. Çelebi, K. Pekmez, H. Özyörük and A. Yıldız, *Catal. Commun.*, 2008, **9**, 2175.
- 17 F. Li, B. Zhang, S. Dong and E. Wang, *Electrochim. Acta*, 1997, **42**, 2563.
- 18 D. J. Guo and H. L. Li, *J. Colloid Interface Sci.*, 2005, **286**, 274.
- 19 D. J. Guo and H. L. Li, *Electrochem. Commun.*, 2004, **6**, 999.
- 20 I. P. Beletskaya, A. N. Kashin, I. A. Khotina and A. R. Khokhlov, *Synlett*, 2008, 1547.
- 21 J. Cookson, *Platinum Met. Rev.*, 2012, **56**, 83.
- 22 G. Nie, X. Lu, J. Lei, L. Yang, X. Bian, Y. Tong and C. Wang, *Electrochim. Acta*, 2013, **99**, 145.
- 23 X. Chena, Z. Caid, Z. Huang, M. Oyamac, Y. Jiang and X. Chen, *Electrochim. Acta*, 2013, **97**, 398.

Received: 20th September 2013; Com. 13/4208